

SUPPORTING INFORMATION

Energy Transfer Cassettes In Silica Nanoparticles Target Intracellular Organelles

*Jiney Jose,^a Aurore Loudet,^a Yuichiro Ueno,^a Liangxing Wu,^a Hsiang-Yun Chen,^a Dong
Hee Son,^a*

Rola Barhoumi,^b Robert Burghardt^b and Kevin Burgess^a*

^aDepartment of Chemistry, Texas A & M University, Box 30012, College Station, TX
77841; ^bDepartment of Veterinary Integrative Bioscience, Texas A & M University, Box
30012, College Station, TX 77843

E-mail: burgess@tamu.edu

Tel: +1 979 845-4345; Fax: +1 979 845-8839; E-mail: burgess@tamu.edu

TABLE OF CONTENTS

A.	General Experimental Methods	3
B.	Photophysical Properties and Determination of Quantum Yields.....	4
C.	Syntheses and NMR, MS spectra of the Cassettes.....	5
	<i>Cassette 1</i>	5
	<i>Cassette 2</i>	8
D.	Structures of The Through-bond Energy Transfer Cassettes Encapsulated In Silica Nanoparticles	11
E.	Structures of The Corresponding Acceptors Encapsulated In Silica Nanoparticles.....	12
F.	General Procedure for Synthesis of Silica Nanoparticles	13
G.	Data For Encapsulation Of Acceptor Fragments For Cassettes 1 and 2	14
H.	Silica Nanoparticle Characterizations.....	16
	<i>Transmission electron microscopy (TEM)</i>	16
I.	Photostability Measurement of Silica Nanoparticles	18
J.	In vitro Cellular Imaging Studies	19
	<i>Cell Culture</i>	19
	<i>Fluorescence microscopy</i>	19
	<i>Fluorescence microscopy for cassette 1-SiO₂ nanoparticles (refers to Figure 3a-b in article).</i>	19
	<i>Fluorescence microscopy for 2-SiO₂ nanoparticles (refers to Figure 4a-b in article).</i>	21
	<i>Fluorescence microscopy for acceptor1-SiO₂ nanoparticles (refers to Figure 5-left in article).</i>	22
	<i>Fluorescence microscopy for acceptor2-SiO₂ nanoparticles (refers to Figure 5-right in article).</i>	25
K.	Transmission Electron Microscopy (TEM) Studies.....	27

A. General Experimental Methods

All reactions were carried out under an atmosphere of dry nitrogen. Glassware were oven-dried prior to use. Unless otherwise indicated, common reagents or materials were obtained from commercial source and used without further purification. All solvents were dried prior to use with appropriate drying agents. Dry distilled DMF was obtained from Acros and used as such. Flash column chromatography was performed using silica gel 60 (230-400 mesh). Analytical thin layer chromatography (TLC) was carried out on Merck silica gel plates with QF-254 indicator and visualized by UV. Fluorescence spectra were obtained on a Varian Cary Eclipse fluorescence spectrophotometer at room temperature. Absorbance spectra were obtained on a Varian 100 Bio UV-Vis spectrophotometer at room temperature. IR spectra were recorded on a Bruker Tensor 27 spectrometer. X-ray photoelectron spectroscopy (XPS) was performed using a Kratos Axis Ultra Imaging X-ray photoelectron spectrometer.

B. Photophysical Properties and Determination of Quantum Yields

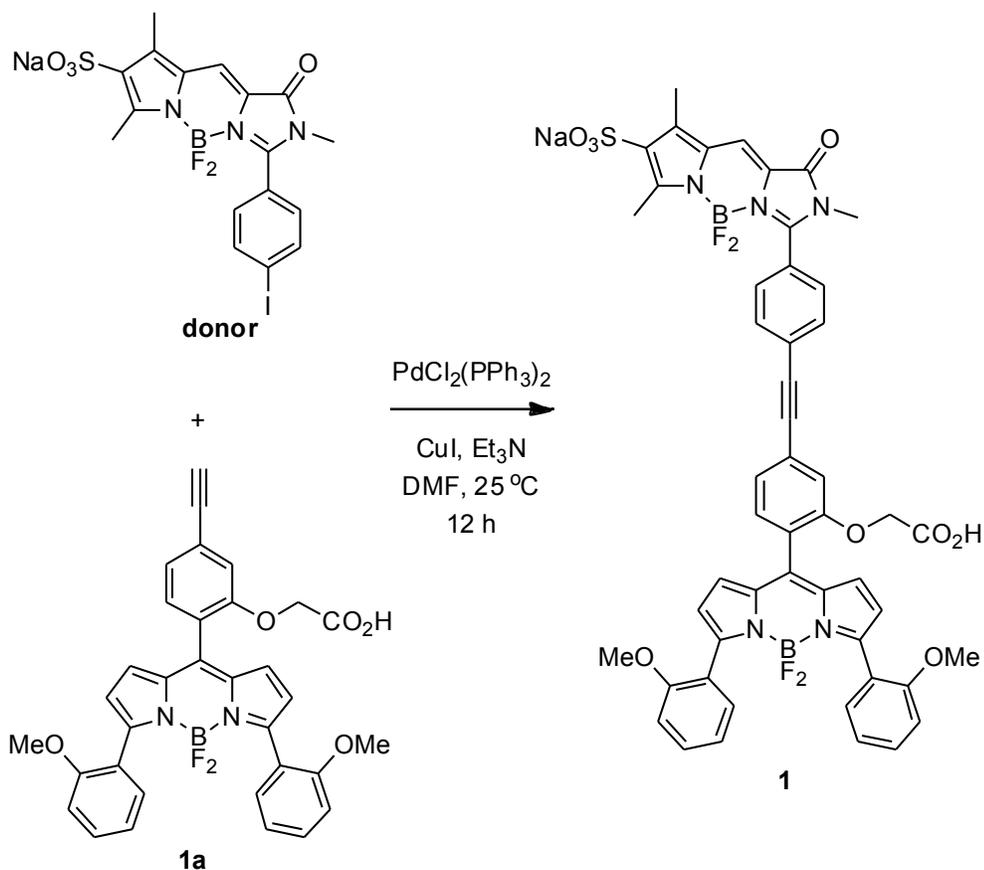
Steady-state fluorescence spectroscopic studies were performed on a Cary Eclipse fluorometer. The slit width was 5 nm for both excitation and emission. The relative quantum yields of the samples were obtained by comparing the area under the corrected emission spectrum of the test sample with that of a standard dye.¹ The quantum efficiencies of fluorescence were obtained from three measurements with the following equation:

$$\Phi_x = \Phi_{st} (I_x/I_{st}) (A_{st}/A_x) (\eta_x^2/\eta_{st}^2)$$

Where Φ_{st} is the reported quantum yield of the standard, I is the area under the emission spectra, A is the absorbance at the excitation wavelength and η is the refractive index of the solvent used, measured on a pocket refractometer from ATAGO. X subscript denotes unknown, and st denotes standard.²

C. Syntheses and NMR, MS spectra of the Cassettes.

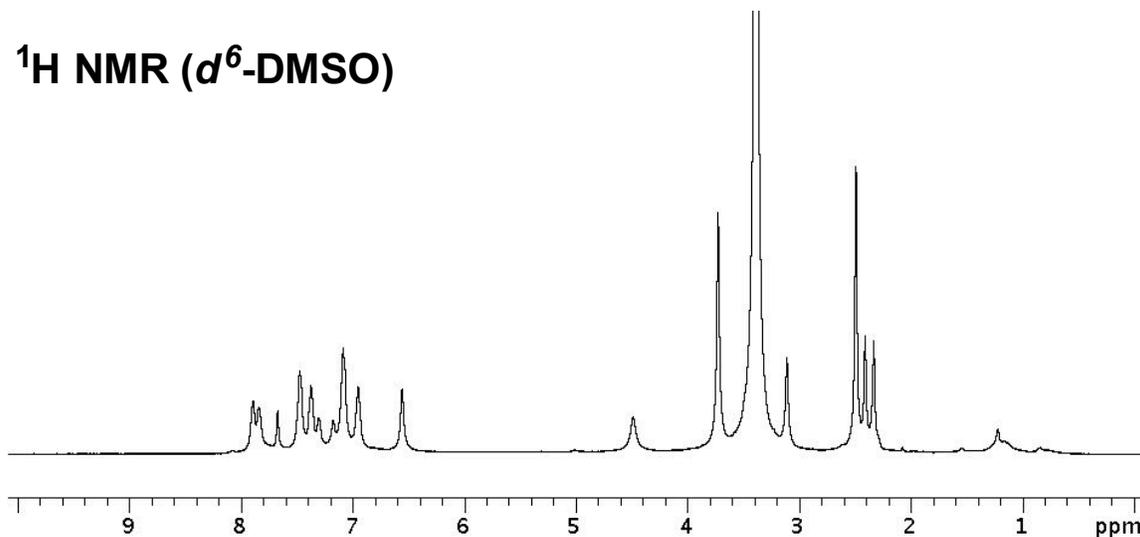
Cassette 1



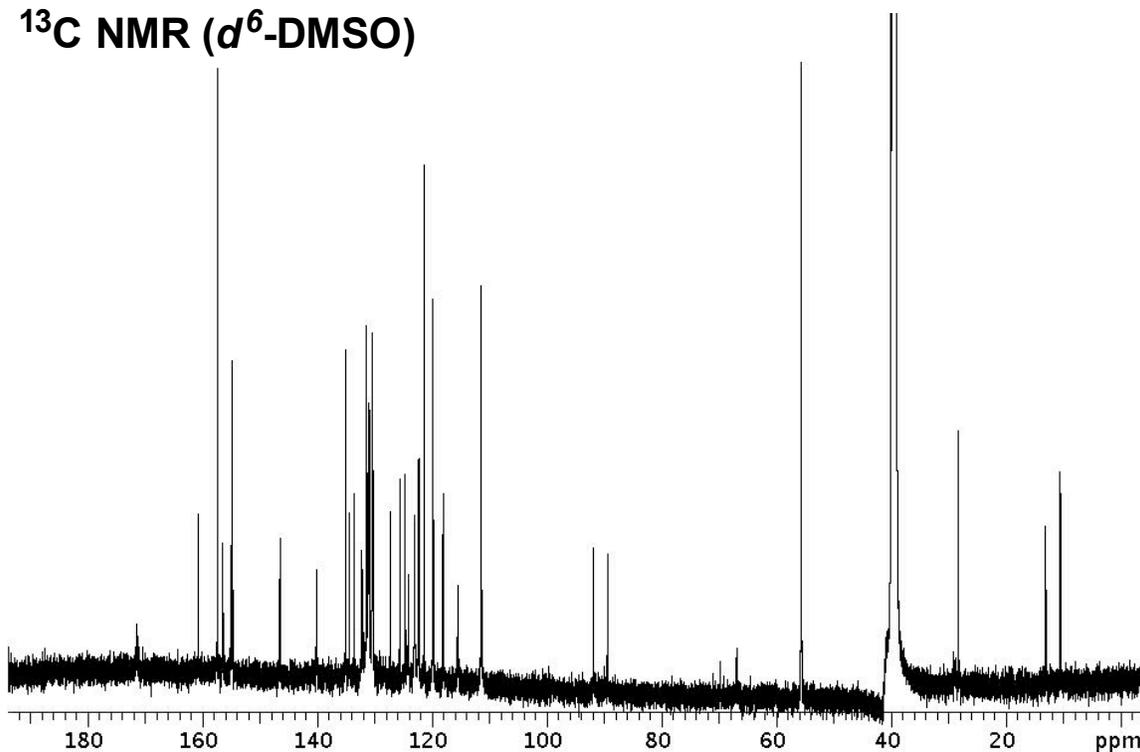
A solution of donor (14 mg, 0.025 mmol), BODIPY acceptor **1a** (20 mg, 0.035 mmol), $\text{PdCl}_2(\text{PPh}_3)_2$ (2 mg, 0.003 mmol) and CuI (0.6 mg, 0.003 mmol) in 3 mL DMF was degassed and filled with N_2 then Et_3N (35 μL , 0.25 mmol) was added. The reaction mixture was stirred at $25\text{ }^\circ\text{C}$ for 24 h then concentrated under reduced pressure. The residue was purified by flash chromatography (20 % $\text{MeOH}/\text{CH}_2\text{Cl}_2$) to afford the product **1** (20 mg, 79 %) as a red solid. ^1H NMR (500 MHz, d^6 - DMSO) δ 7.89-7.84 (m, 3H), 7.67 (s, 1H), 7.47 (br, 3H), 7.37-7.30 (m, 4H), 7.17 (s, 1H), 7.08-7.07 (m, 4H), 6.95 (br, 2H), 6.56 (br, 2H), 4.48 (s, 2H), 3.73 (s, 6H), 3.11 (s, 3H), 2.41 (s, 3H), 2.33 (s, 3H); ^{13}C NMR (500 MHz, d^6 - DMSO) δ 171.3, 160.7, 157.3, 156.4, 155.0, 154.7, 146.4, 140.1, 140.0, 135.0, 134.4, 133.5, 132.2, 131.4, 131.1, 130.9, 130.4, 130.2, 127.2, 125.6, 124.6,

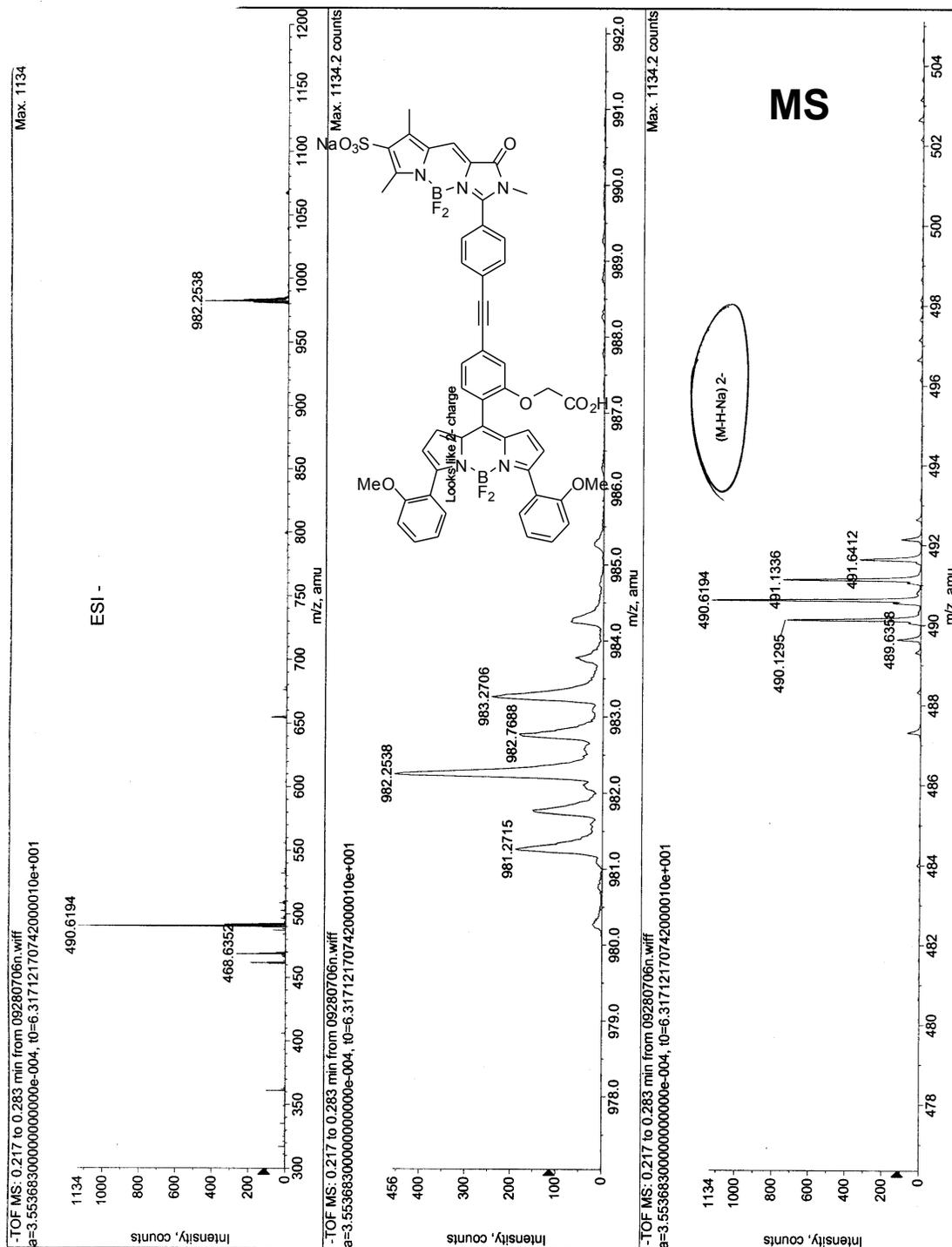
124.1, 123.0, 122.3, 121.3, 119.8, 118.1, 117.9, 115.5, 111.4, 91.8, 89.4, 66.9, 55.6, 28.2, 13.0, 10.5; MS (ESI) m/z calcd for $(M-Na)^-$ $C_{50}H_{38}B_2F_4N_5O_9S$ 982.25; found 982.25. m/z calcd for $(M-Na-H)^{2-}$ $C_{50}H_{37}B_2F_4N_5O_9S$ 490.62; found 490.62.

1H NMR (d^6 -DMSO)

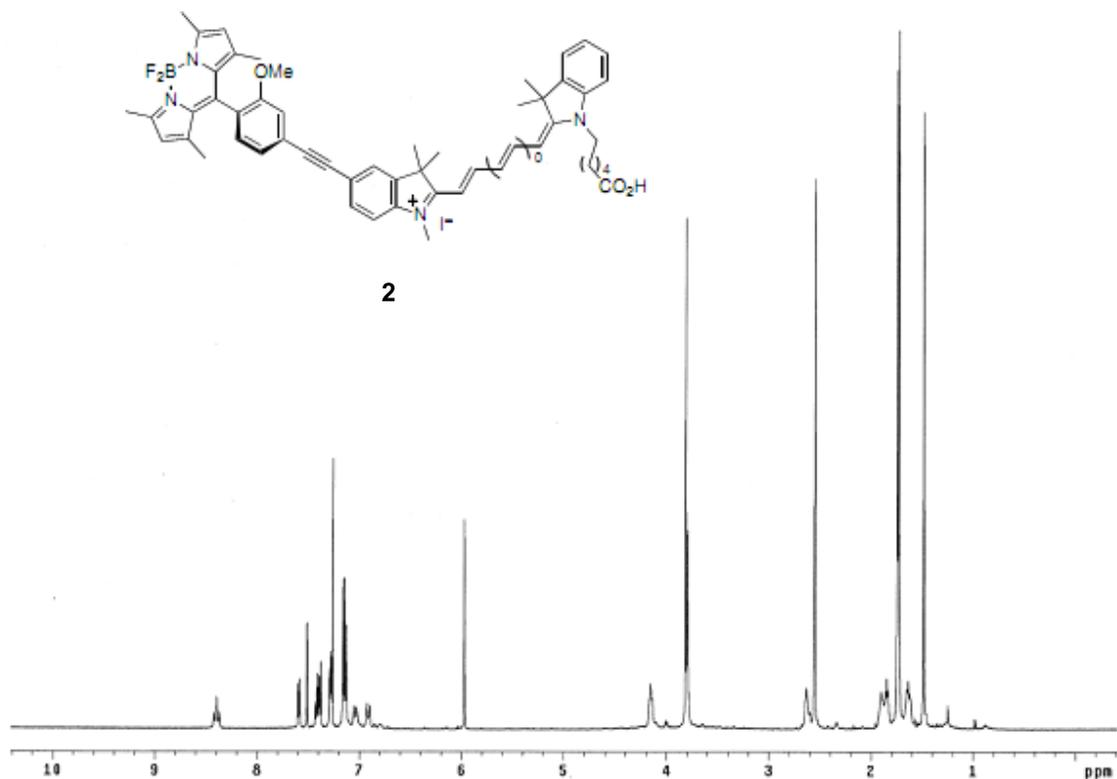


^{13}C NMR (d^6 -DMSO)

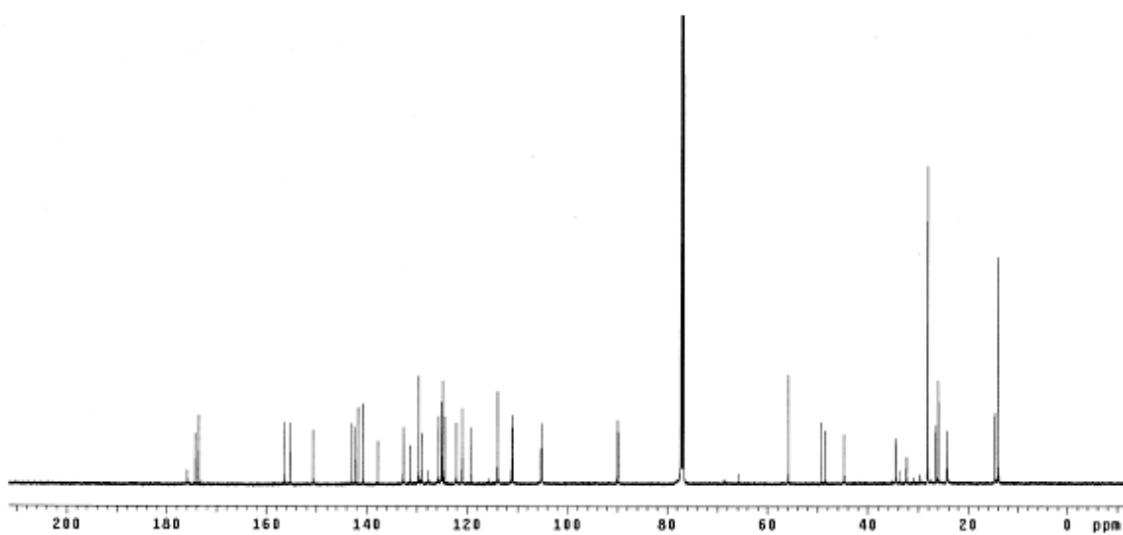




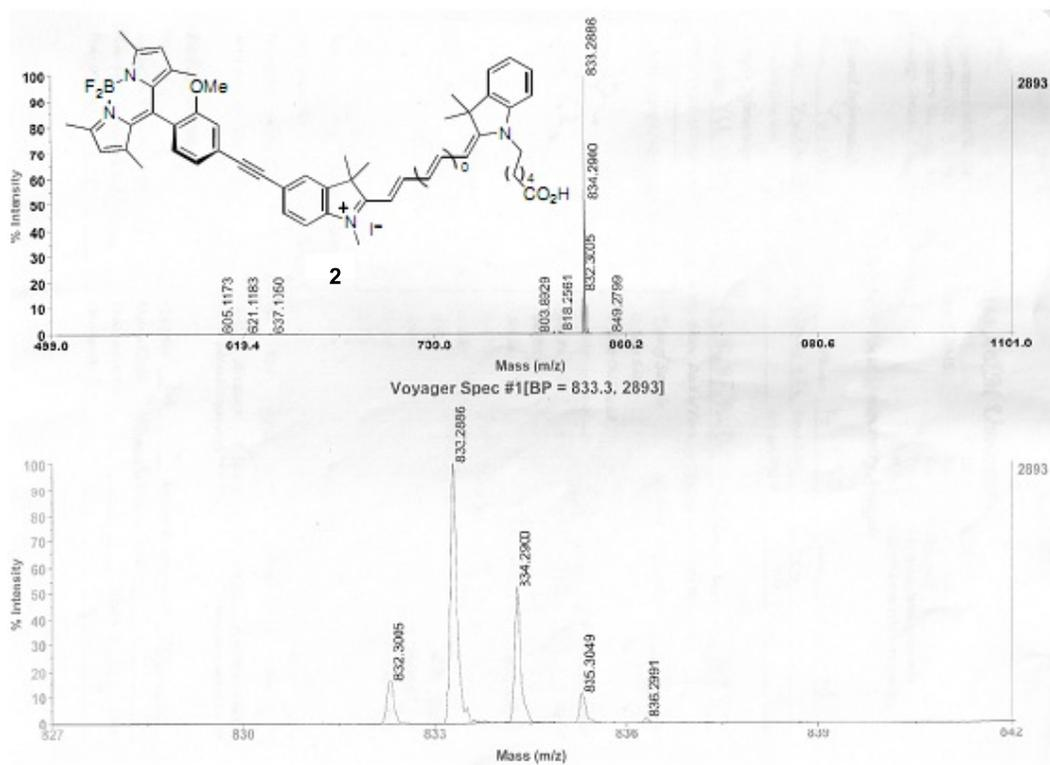
114.0, 111.2, 110.9, 105.3, 105.1, 90.0, 89.8, 55.8, 49.2, 48.6, 44.7, 34.5, 32.3, 28.16, 28.13, 26.5, 26.0, 24.2, 14.6, 14.0; MS (MALDI) m/z 833.29 (M)⁺.



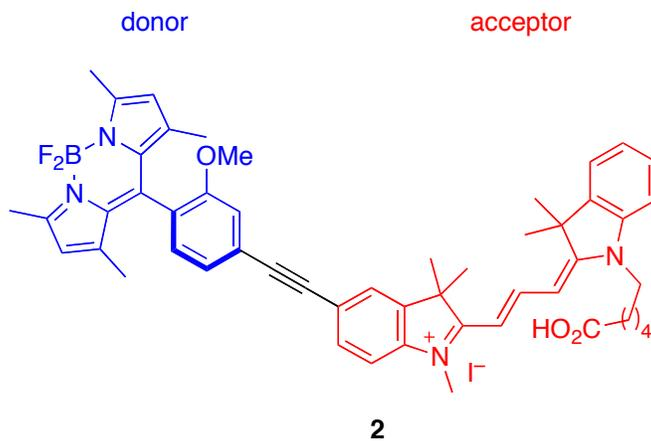
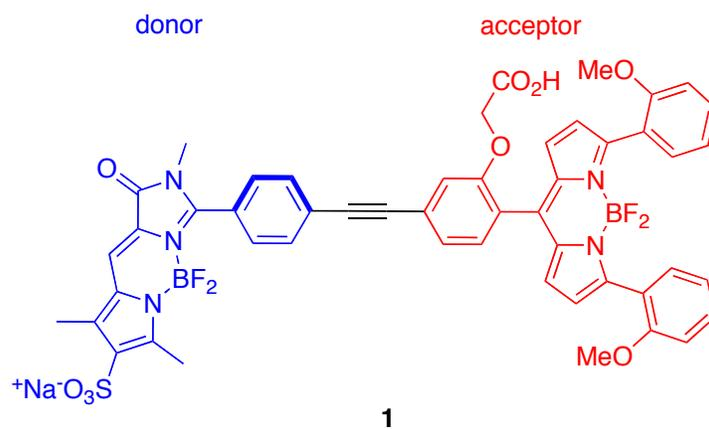
¹H NMR (CDCl₃)



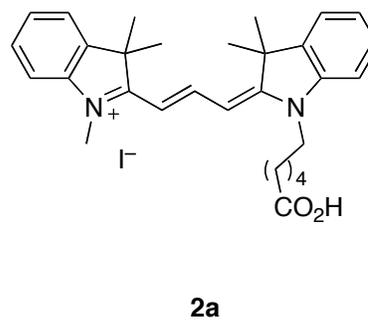
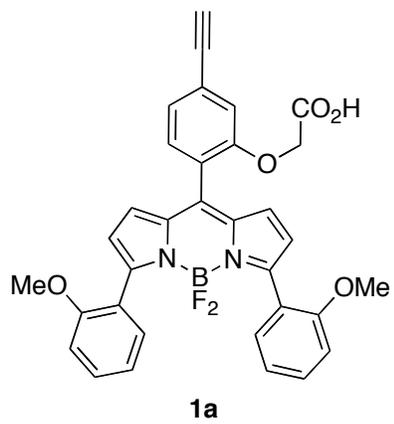
¹³C NMR (CDCl₃)



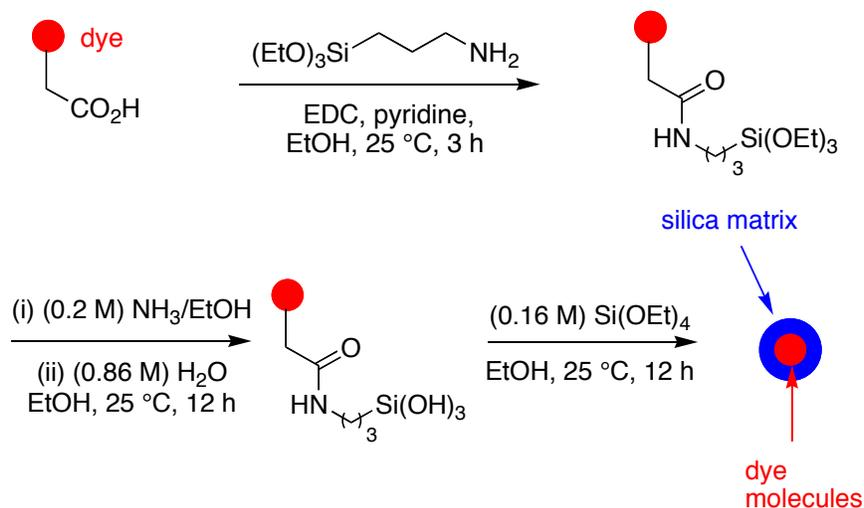
D. Structures of The Through-bond Energy Transfer Cassettes Encapsulated In Silica Nanoparticles



E. Structures of The Corresponding Acceptors Encapsulated In Silica Nanoparticles



F. General Procedure for Synthesis of Silica Nanoparticles



The encapsulation of cassettes and corresponding acceptors were achieved by following a reported procedure by Wiesner *et al* with slight modification.³ The organic dye is conjugated via activated carboxylic acid group to 3-aminopropyltriethoxysilane (APTS) at a molar ratio of 1:50 (fluorophore:APTS) in degassed absolute EtOH (1.0 mL, 200 proof) under nitrogen. The above dye solution (0.14 mL, $1.7 \times 10^{-5}\text{ M}$) was added to EtOH (200 % proof) along with deionized water (1.52 mL, 0.86 M) and NH_3 in EtOH (5.0 mL, 0.2 M) at $25\text{ }^\circ\text{C}$ to make up a final volume of 50 mL and stirred for 12 h at $25\text{ }^\circ\text{C}$. TEOS (1.63 mL, 0.16 M) was then added in aliquots of 0.4 mL every fifteen minutes and stirring continued for another 12 h at $25\text{ }^\circ\text{C}$. The resulting silica nanoparticles were dialyzed into EtOH to removed unreacted starting materials using a Spectra/Por dialysis membrane with molecular weight cut off (MWCO) 6000-8000 for 12 h. Further dialysis was performed to transfer the formed silica nanoparticles from EtOH to deionized water and finally to pH 7.4 (0.1 M sodium phosphate buffer).

G. Data For Encapsulation Of Acceptor Fragments For Cassettes 1 and 2

Acceptor **1a** encapsulated in silica had low quantum yield in EtOH and pH 7.4 compared to free acceptor. For acceptor **2a** (Cy3) encapsulated in silica, the quantum yield was slightly higher in EtOH and almost 9 fold higher in pH 7.4 compared to free acceptor (Table 1).

In case of cassette **1** encapsulated in silica, the quantum yields when excited at donor and acceptor were lower than free cassette in EtOH and pH 7.4. For cassette **2** encapsulated in silica, the quantum yields when excited at donor and acceptor was slightly higher in EtOH and very low in pH 7.4 compared to free cassette **2** in respective solvents (Table 2). Thus we do find change in spectral properties (quantum yield) of silica nanoparticles in different solvents. I am not sure whether we can correlate the spectral changes of acceptor encapsulated silica and cassette encapsulated silica because cassette is much bigger than the acceptor. Thus acceptor may be more efficiently encapsulated and therefore show an increase or only slight decrease in quantum yields whereas cassettes may less efficiently encapsulated and therefore shows decrease in quantum yields and energy transfer.

Table S1. Photophysical properties of bare acceptors and silica encapsulated acceptors in different solvents.

dye	solvent	$\lambda_{\max \text{ abs}}$ (nm)	$\lambda_{\max \text{ emiss}}$ (nm)	fwhm (nm)	Φ
1a	EtOH	548	602	51	0.48+/-0.01 ^b
Si-1a	EtOH	548	601	47	0.36+/-0.02
Si-1a	pH 7.4 ^a	548	601	49	0.32+/-0.01
2a	EtOH	549	565	35	0.085 ^c
2a	pH 7.4 ^a	542	567	37	0.039
Si-2a	EtOH	550	566	38	0.091
Si-2a	pH 7.4 ^a	550	566	37	0.30+/-0.02

Si: silica encapsulation. ^a0.1 M sodium phosphate buffer. Standard for quantum yield measurements: ^brhodamine 6G (Φ 0.95 in EtOH); ^crhodamine 101 (Φ 1.0 in EtOH). Quantum yields were measured three times and averaged.

Table S2. Photophysical properties of bare cassettes and silica encapsulated cassettes in different solvents.

dye	solvent	$\lambda_{\max \text{ abs}}$ (nm)	$\lambda_{\max \text{ emiss}}$ (nm)	Φ^b <i>ex. at donor</i>	Φ <i>ex. at acceptor</i>	ETE (%)
1	EtOH	498, 543	600	0.46+/-0.02	0.48+/-0.01 ^b	96
Si-1	EtOH	492, 542	600	0.36+/-0.03	0.37+/-0.02	97
Si-1	pH 7.4 ^a	499, 544	597	0.31+/-0.02	0.33+/-0.01	93
2	EtOH	504, 569	590	0.20+/-0.01	0.22+/-0.02 ^c	90
Si-2	EtOH	502, 571	594	0.23+/-0.01	0.25+/-0.02	92
Si-2	pH 7.4 ^a	504, 568	592	0.04	0.05	78

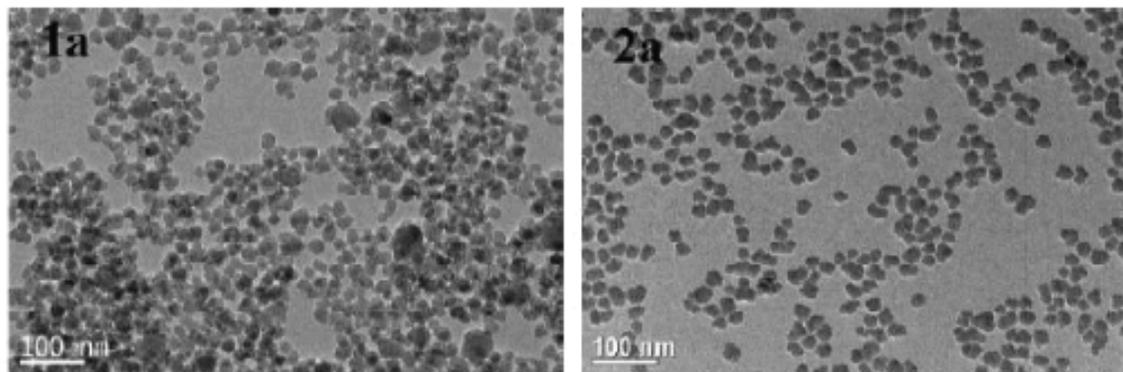
Si: silica encapsulation. ^a0.1 M sodium phosphate buffer. Standard for quantum yield measurements: ^brhodamine 6G (Φ 0.92 in EtOH); ^crhodamine 101 (Φ 1.0 in EtOH). Quantum yields were measured three times and averaged.

H. Silica Nanoparticle Characterizations

Transmission electron microscopy (TEM)

Sample preparation and measurement: A few drops of silica nanoparticles in ethanol were placed on a TEM grid. The TEM grid is made of copper meshes and covered with a thin film of amorphous carbon. The grid is dried and mounted on a specimen holder and loaded on to the TEM. Measurements were made on a JEOL 2010 TEM instrument. The JEOL 2010 is fitted with a LaB₆ thermal emission gun and a Gatan Sc1000 ORIUS slow-scan charge-coupled device (CCD) camera (Model 832 with 4008x2672 pixels). Bright filed TEM images were obtained with JEOL 2010.

a



b

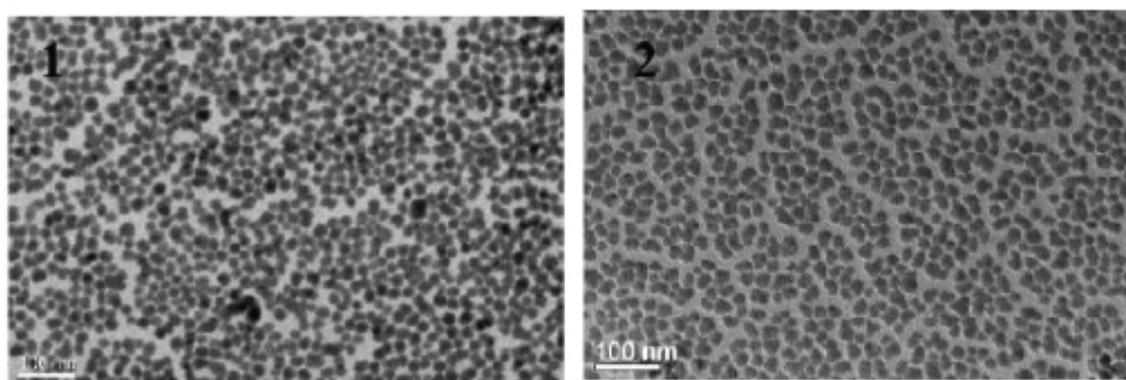


Figure S1. Transmission electron microscope (TEM) images of (a) acceptors **1a-2a** and (b) cassettes **1-2**; particle size: 20-24 nm.

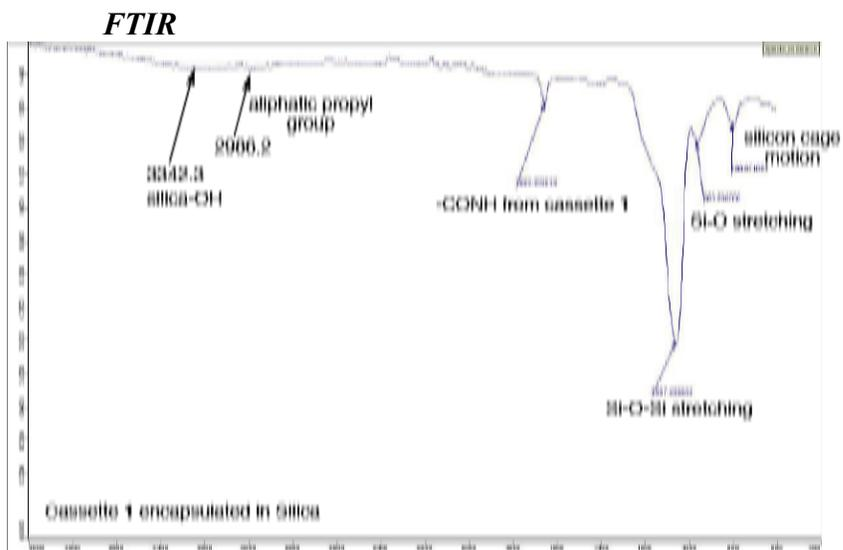


Figure S2. FTIR spectra of cassette 1 doped silica nanoparticles.

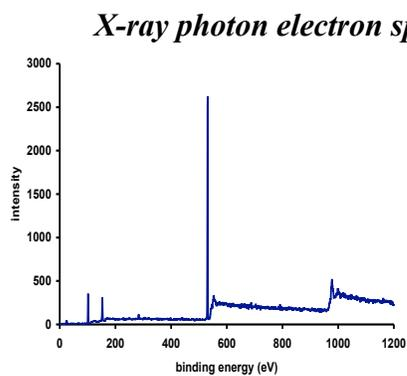


Figure S3. X-ray photon electron spectroscopy (XPS) whole range spectrum of cassette 1 doped silica nanoparticles.

I. Photostability Measurement of Silica Nanoparticles

The photostability measurements of the silica nanoparticles were performed in the dry state. A few drops of silica nanoparticle suspension (1mg/mL) or dye in ethanol (concentration 10^{-6} M) were placed on a 2 x 2 cm glass slide and air dried. An argon ion laser (Spectra-Physics) fitted with notch filter to remove 514 nm wavelength light was used to perform the photostability studies. The 488 nm wavelength light with power density (5.85 W/cm^2) was focused on the dried sample on the glass slide. A biconvex lens was used to concentrate the beam on the sample. The fluorescence output from the sample upon irradiation was collected using an objective lens. The collected fluorescence output was passed through a filter to remove any stray light below 500 nm and to a collimator that was connected to a charged coupled device (CCD) detector (Ocean Optics), which was maintained at $-10 \text{ }^\circ\text{C}$.

J. In vitro Cellular Imaging Studies

Cell Culture

Clone 9 normal rat liver cells (American Type Culture Collection) were cultured as subconfluent monolayers on 75 cm² culture flask with vent caps in Ham's medium supplemented with 10 % fetal bovine serum (FBS) in a humidified incubator at 37 °C with 5 % CO₂. Cells grown to subconfluence were enzymatically dissociated from the surface with trypsin and plated 2-3 days prior to the experiments in Lab-Tek two well chambered coverglass slides (Nunc).

Fluorescence microscopy

Uptake and subcellular localization of the cassette doped silica nanoparticles **1-SiO₂**, **2-SiO₂**, **1a-SiO₂**, and **2a-SiO₂** were studied on living Clone 9 normal rat liver cells using a Zeiss 510 META NLO Multiphoton Microscope System consisting of an Axiovert 200 MOT microscope. Throughout, digital images were captured with a 40x / 1.3 oil objective with the following filter sets:

- for nanoparticles **1-SiO₂**, and **2-SiO₂**: Excitation 488 nm; Emission BP 500-530 for the donor part ; Emission BP 565-615 for the acceptor part
- for ER-Tracker™ Blue-White DPX : Excitation 740 nm; Emission BP 435 - 485
- for LysoTracker® Green DND-26 : Excitation 488 nm; Emission BP 500-530
- for MitoTracker® Deep Red: Excitation 633 nm; Emission BP 650-710
- for nanoparticles **1a-SiO₂**, and **2a-SiO₂** : Excitation 543 nm; Emission BP 565-615

Fluorescence microscopy for cassette 1-SiO₂ nanoparticles (refers to Figure 3a-b in article).

Clone 9 cells were incubated for 2 hours at 37 °C in serum free culture medium with 0.01 mg/mL (10 µL) of doped nanoparticles (1 mg/mL stock solution in PBS 7.4)). After the incubation period, the cells were washed with serum free culture medium several times before imaging.

To confirm the subcellular localization of the nanoparticles, Clone 9 cells pre-treated with **1-SiO₂** were co-incubated with 0.5 μM ER-Tracker™ Blue-White DPX (1 mM stock solution, Invitrogen®) in HBSS with Calcium and Magnesium for 30 min at 37 °C (Figure S4).

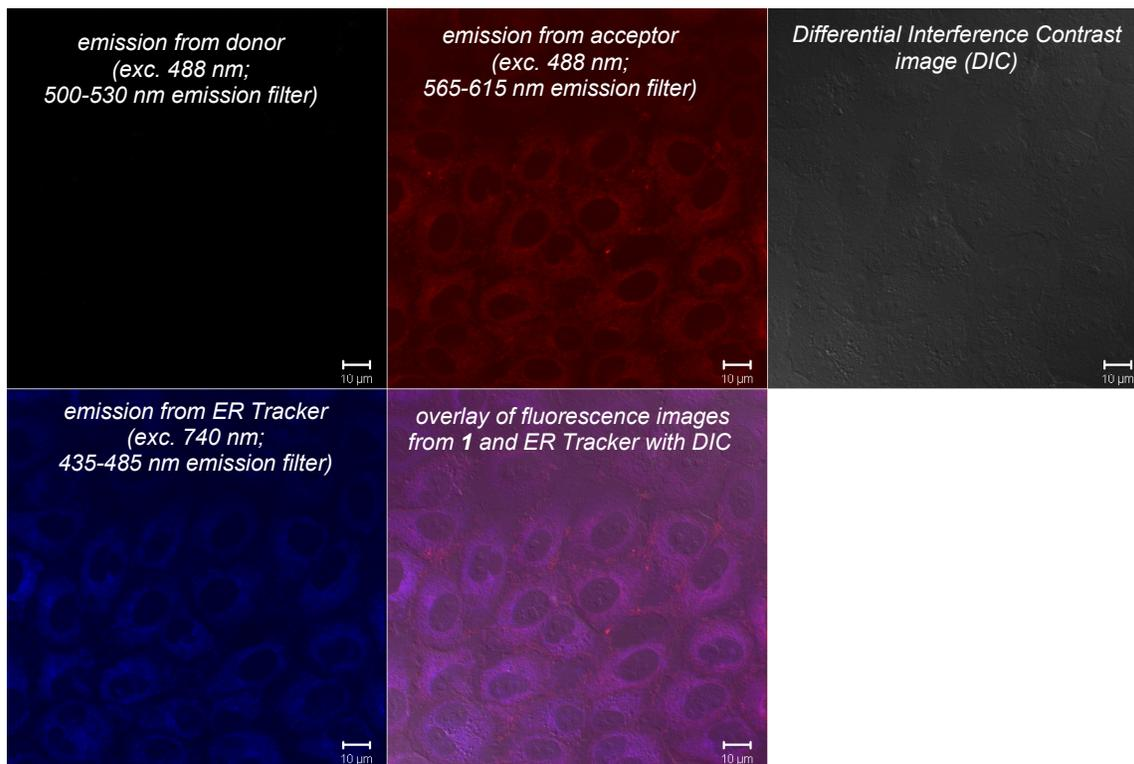


Figure S4. Cellular uptake of **1-SiO₂** (10 μL) and co-localization with ER-Tracker™ Blue-White DPX.

Fluorescence microscopy for 2-SiO₂ nanoparticles (refers to Figure 4a-b in article).

Clone 9 cells were incubated for 2 hours at 37 °C in serum free culture medium with 0.01 mg/mL (10 μL) of doped nanoparticles (solution in PBS). After the incubation period, the cells were washed with serum free culture medium several times before imaging.

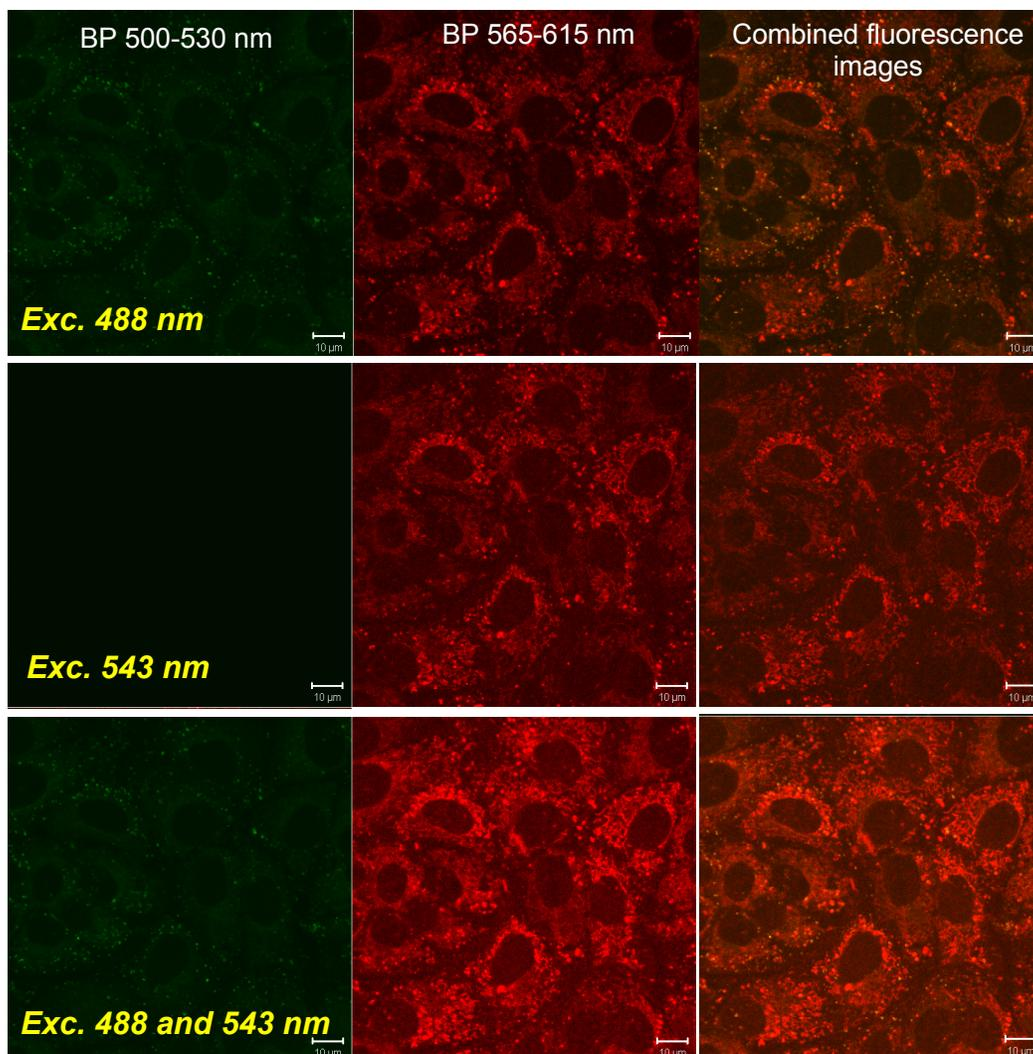


Figure S5. Cellular uptake of 2-SiO₂. In the top panel, the cells were excited at 488 nm; 2-SiO₂ accumulated in the lysosomes and/or endosomes (green/red) and the mitochondria (red). In the middle panel, the cells were excited at 543 nm (acceptor part). The bottom panel is upon excitation at both 488 and 543 nm.

Fluorescence microscopy for *acceptor1-SiO₂* nanoparticles (refers to Figure 5-left in article).

Clone 9 cells were incubated for 2 hours at 37 °C in Ham's medium (supplemented with 10% FBS) with 2 μL of doped nanoparticles (EtOH stock solution). After the incubation period, the cells were washed with serum free culture medium several times before imaging.

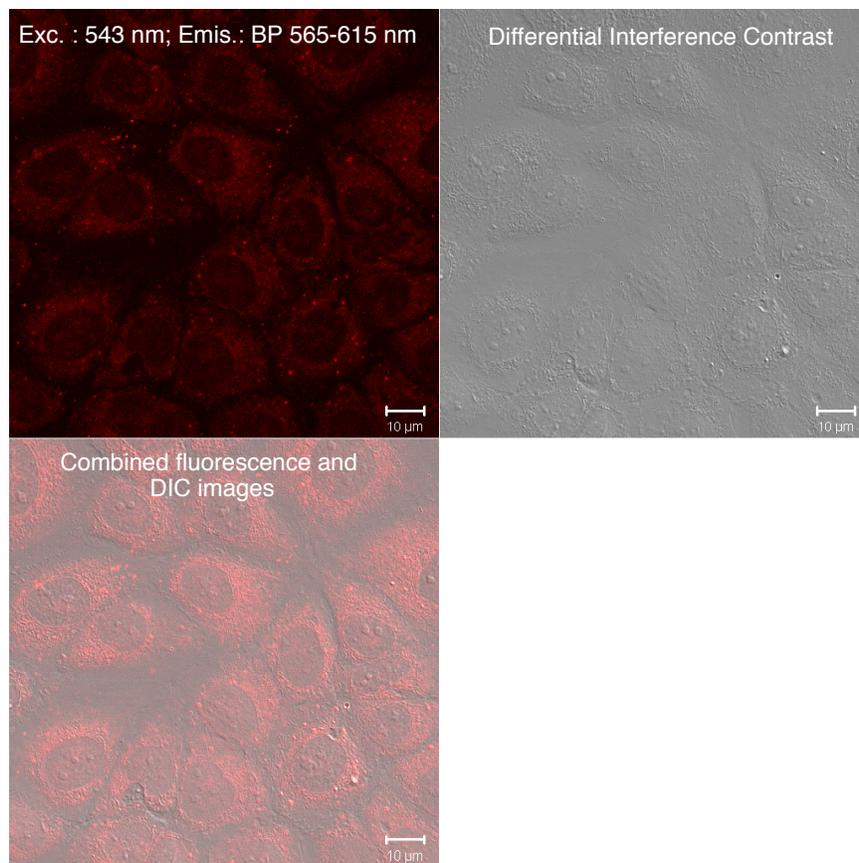


Figure S6. Cellular uptake of **acceptor 1-SiO₂** in Clone 9 cells. Cells were excited at 543 nm; Emission was detected with a BP BP 565-615

To confirm the subcellular localization of the nanoparticles, Clone 9 cells pre-treated with **acceptor1-SiO₂** were co-incubated with 100 nM LysoTracker Green for 30 min at 37 °C (Figure S7). Thereafter, the same cells were treated with 0.5 μM ER-Tracker™ Blue-White DPX (1 mM stock solution, Invitrogen®) in HBSS with Calcium and Magnesium for 30 min at 37 °C (Figure S8).

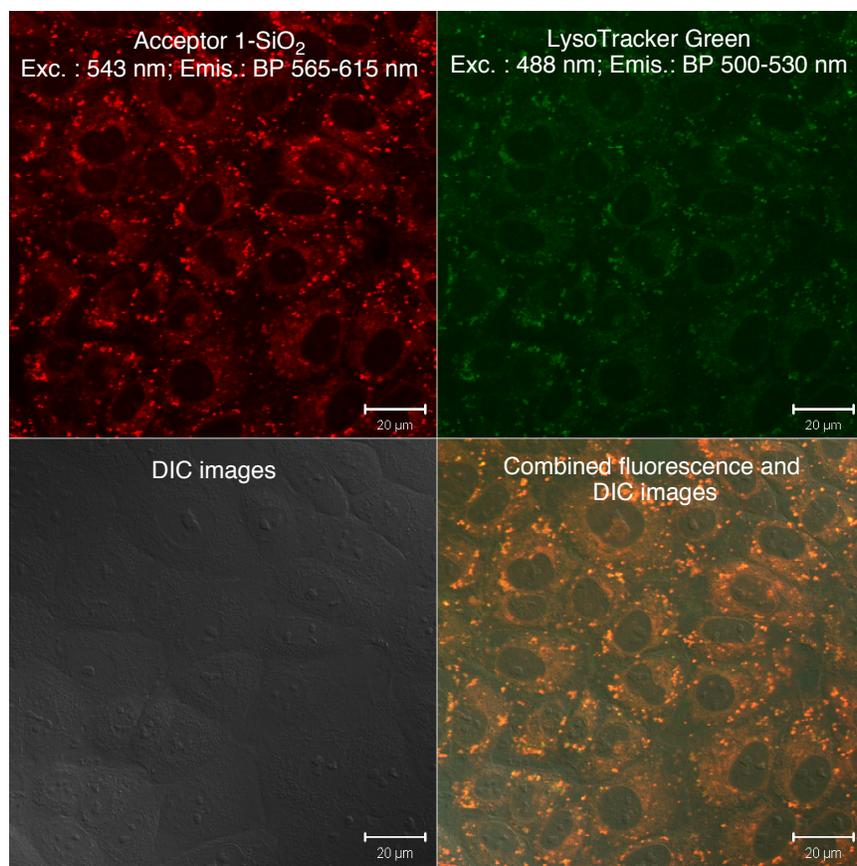


Figure S7. Cellular uptake of **acceptor 1-SiO₂** and co-localization with Lyso-Tracker™ Green.

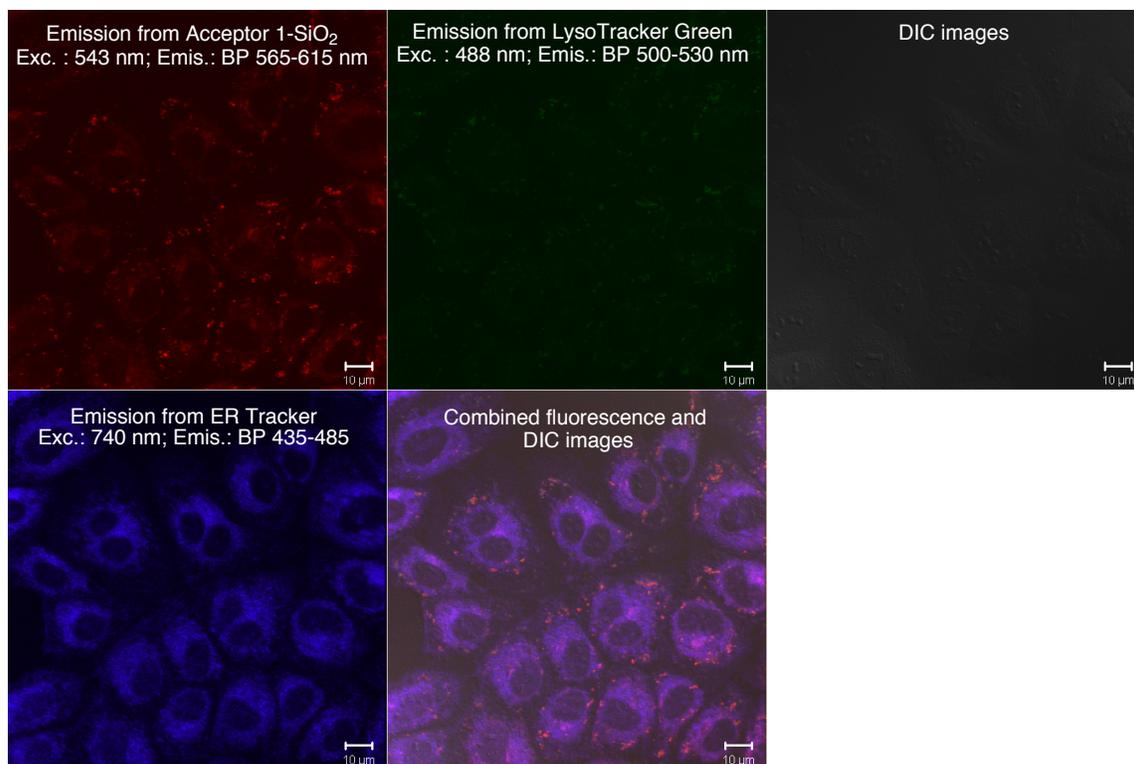


Figure S8. Cellular uptake of **acceptor 1-SiO₂** and co-localization with ER-Tracker™ Blue-White DPX after the cells were pre-treated with Lyso-Tracker Green.

Fluorescence microscopy for *acceptor2-SiO₂* nanoparticles (refers to Figure 5-right in article).

Clone 9 cells were incubated for 2 hours at 37 °C in Ham's medium (supplemented with 10% FBS) with 20 µL of doped nanoparticles (stock solution in PBS pH 7.4). After the incubation period, the cells were washed with serum free culture medium several times before imaging.

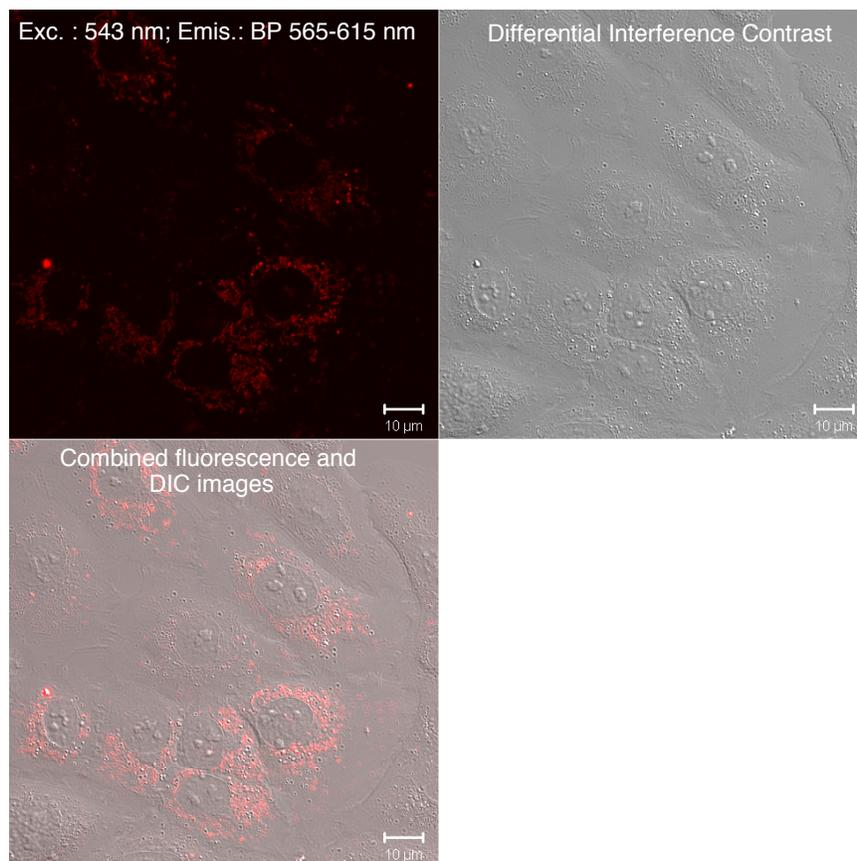


Figure S9. Cellular uptake of **acceptor 2-SiO₂** in Clone 9 cells. Cells were excited at 543 nm; Emission was detected with a BP BP 565-615.

Subcellular localization of the nanoparticles into the mitochondria was confirmed by comparing the staining pattern of Clone 9 cells that were treated with 100 nM MitoTracker® Deep Red for 10 min at 37 °C (Figure S10) to the one treated with *acceptor 2-SiO₂*.

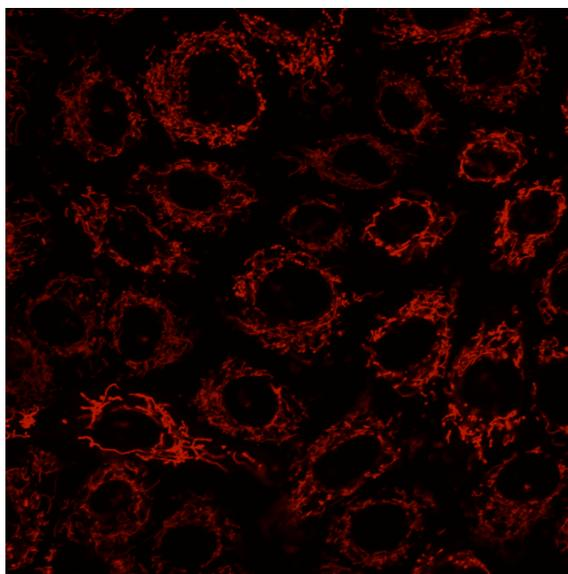


Figure S10. Cellular uptake of **MitoTracker Deep Red** in Clone 9 cells. Cells were excited at 633 nm; Emission was detected with a BP 650-710.

K. Transmission Electron Microscopy (TEM) Studies

To confirm the uptake of the silica nanoparticles, TEM was only done once on Clone 9 cells that were treated with **1a-SiO₂** for 2 h (Ham's medium). TEM analysis shows internalization of the nanoparticles into intracytoplasmic vacuoles or endosomes, as well as free in the cytoplasm, suggesting that they are able to escape from the endosomes and resist degradation.

Clone 9 cells were grown in 2-well glass chamber slides (LabTek type I) in Ham's medium supplemented with 10% FBS. The cells were treated with 2 $\mu\text{L}/\text{mL}$ of doped nanoparticles (EtOH stock solution) for 2 hours at 37 °C in Ham's medium. After the incubation period, the cells were washed, detached by trypsinization, sedimented in small diameter micro centrifuge tubes and fixed in 2% glutaraldehyde, 2% formaldehyde in 0.1M Na cacodylate buffer. The aldehyde-fixed samples were washed in 0.1M sodium cacodylate buffer, postfixed for 1 h in 1% osmium tetroxide reduced with 0.5% potassium ferrocyanide in 0.1M sodium cacodylate buffer, dehydrated in a graded alcohol series, and embedded in an EMbed812/ Araldite resin mixture (Electron Microscopy Sciences, Hatfield, PA). Ultrathin sections were cut with a Leica EM UC6 microtome, and post-stained with uranyl acetate and lead citrate. Ultrathin sections were examined with a Phillips Morgagni 268 (FEI company, Hillsboro, OR) transmission electron microscope at an accelerating voltage of 80 kV. Digital images were recorded with a MegaViewIII digital camera operated with iTEM software (Olympus Soft Imaging Systems, Germany). Other samples were prepared without potassium ferrocyanide treatment.

TEM studies of Clone 9 cells treated with acceptor 1a-SiO₂

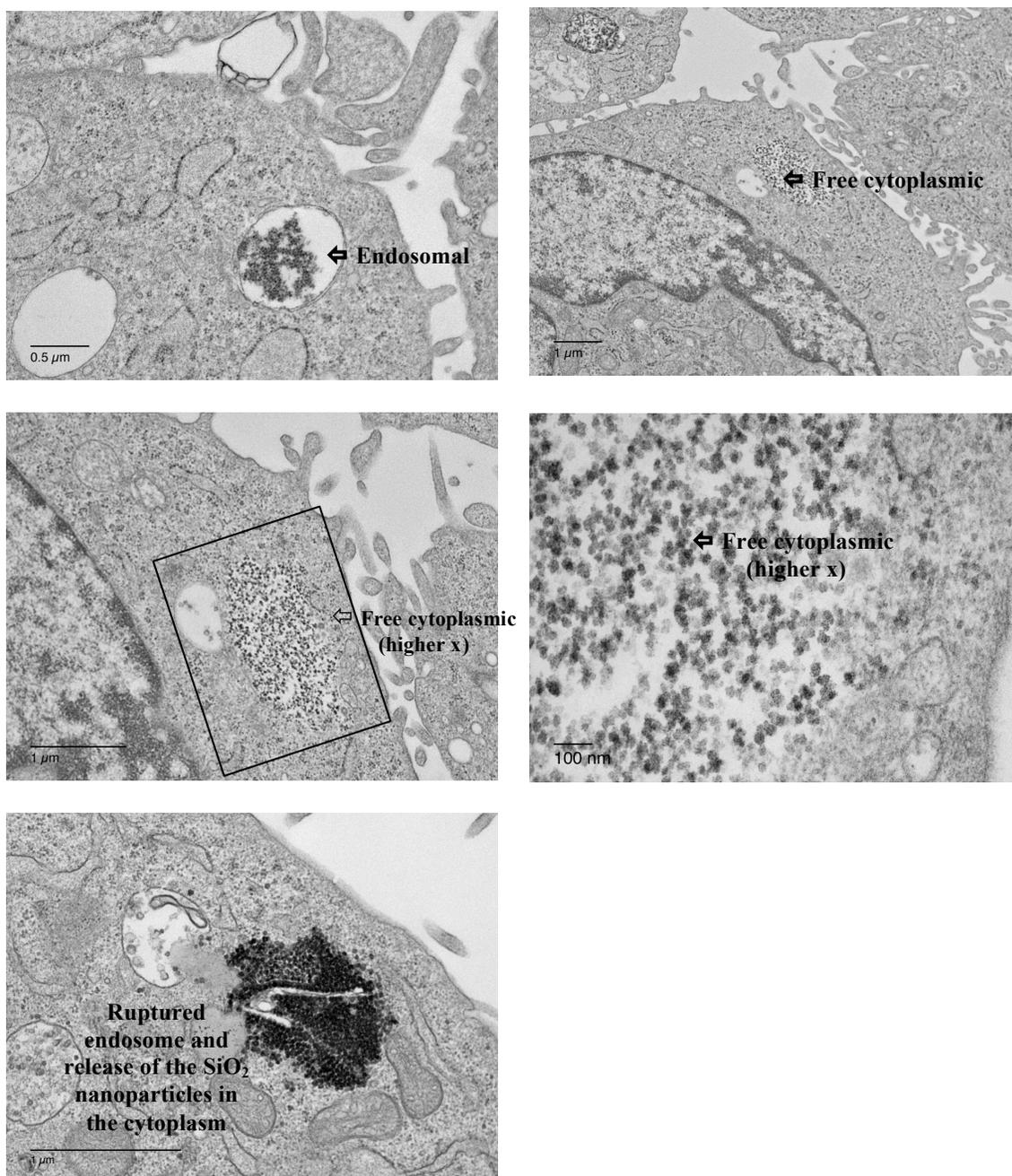


Figure S6. TEM images of Clone 9 cells treated with **1a-SiO₂** showing some of the nanoparticles trapped in endosomes, others free in the cytoplasm, and others escaping from the endosomes.

References

1. K. Rurack, *Springer Ser. Fluoresc.*, 2008, **5**, 101-145.
2. A. T. R. Williams, S. A. Winfield and J. N. Miller, *Analyst* 1983, **108**, 1067-1071.
3. H. Ow, D. R. Larson, M. Srivastava, B. A. Baird, W. W. Webb and U. Wiesner, *Nano. Lett.*, 2005, **5**, 113-117.